NeuroImage 202 (2019) 116051

Contents lists available at ScienceDirect

NeuroImage

journal homepage: www.elsevier.com/locate/neuroimage

Long-term training-dependent representation of individual finger movements in the primary motor cortex

Kenji Ogawa *, Kaoru Mitsui, Fumihito Imai, Shuhei Nishida

Department of Psychology, Hokkaido University, Kita 10, Nishi 7, Kita-ku, Sapporo, 060-0810, Japan

ARTICLE INFO

Keywords:
fMRI
Multi-voxel pattern analysis
Primary motor cortex
Motor learning

ABSTRACT

We investigated the effects of long-term training on the neural representation of individual finger movements in the primary sensorimotor cortex. One group of participants (trained group) included subjects trained in playing the piano (mean years of experience = 17.9; range = 9–26; n = 20). The other group of participants (novice group) had no prior experience (n = 20). All participants performed finger-tapping movements using either of the four digits of the hand (index, middle, ring, and little fingers). Functional magnetic resonance imaging (fMRI) was used to analyze the spatial activation patterns elicited by individual finger movements. Subsequently, we tried to classify the finger that was being moved using a multi-voxel pattern analysis (MVPA). Our results showed significantly higher-than-chance classification accuracies in both primary motor cortex (M1) and somatosensory cortex (S1) contralateral to the hand. We also found significantly lower classification accuracies for both hands in the trained group compared with the novice group in M1, without significant differences in the average signal changes and the number of activated voxels for individual fingers or overlap between digits. Representational similarity analysis (RSA) also demonstrated the differences in similarity patterns of activations between the trained and novice groups in M1. Our results indicate the modulation of neural representations of individual finger movements of M1 due to long-term training.

1. Introduction

The primary sensorimotor cortex contains the topographical map that represents each part of the body, including individual fingers (Penfield and Boldrey, 1937). Studies on monkeys have identified digit maps in the primary somatosensory cortex (S1) (Merzenich et al., 1987; Sur et al., 1982) as well as in the primary motor cortex (M1) (Woolsey et al., 1952). In human S1, neuroimaging studies using functional magnetic resonance imaging (fMRI) (Kolasinski et al., 2016a; Martuzzi et al., 2014; Nelson and Chen, 2008; Overduin and Servos, 2004; Sanchez-Panchuelo et al., 2010; Schweizer et al., 2008; van Westen et al., 2004) or magnetoencephalography (MEG) (Baumgartner et al., 1991; Suk et al., 1991) have revealed somatotopic maps for individual digits. A recent invasive electro-stimulation study also revealed a detailed orderly map of individual fingers in human S1 (Roux et al., 2018). In M1, human neuroimaging studies with fMRI or positron emission tomography (PET) have shown that the neural representations for individual fingers are not distinct but are rather overlapped and distributed (Beisteiner et al., 2001; Dechent and Frahm, 2003; Indovina and Sanes, 2001; Meier et al., 2008; Sanes et al., 1995).

Somatotopic maps are known to be dynamically reorganized based on individual experiences. In S1, both separation and integration of neural representations for individual digits have been reported previously. A MEG study has shown that trained string players exhibit increased distances between activation peaks for specific digit pairs compared with controls (Elbert et al., 1995). Numerous previous studies have individual finger representations in S1 were integrated (or de-differentiated) by intensive training, which could cause a dysfunction in individual finger control (Bara-Jimenez et al., 1998; Butterworth et al., 2003; Catalan et al., 2012; Elbert et al., 1998; Nelson et al., 2009; Weise et al., 2012). Dynamic remapping of somatotopic representations was also found in normal participants owing to learning or tactile stimulation (Braun et al., 2000; Pleger et al., 2003; Schwenkreis et al., 2001). In studies on monkeys, the topological maps in S1 were shown to be modified by intensive tactile training of a fingertip (Jenkins et al., 1990) or by surgical manipulation of artificial syndactyly (Allard et al., 1991). In humans, the topographical finger map is modified after surgical separation of webbed fingers in patients with syndactyly (Mogilner et al., 1993). Further, it has also been shown that a short-term (24 h) gluing manipulation of digits induces reorganization of somatotopy in S1 (Kolasinski et al., 2016b).

* Corresponding author.
E-mail address: ogawa@let.hokudai.ac.jp (K. Ogawa).

https://doi.org/10.1016/j.neuroimage.2019.116051
Received 17 July 2018; Received in revised form 13 June 2019; Accepted 23 July 2019
Available online 24 July 2019

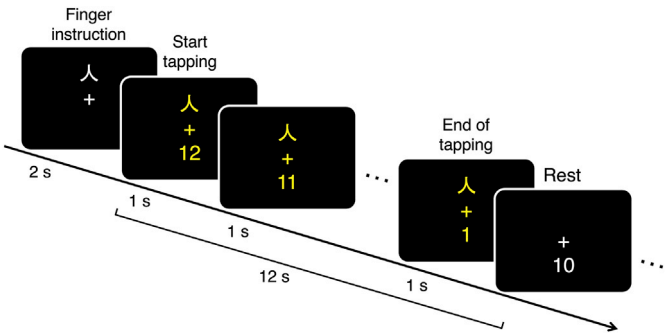

Fig. 1. Schematic depiction of the time course of a single trial. Firstly, the visual cue of a single Japanese character was displayed, indicated by either one among the index, middle, ring, or little fingers. Two seconds later, the color of the fixation cross was changed from white to yellow, followed by displaying the number "12" under the fixation cross. Numbers were counted in reverse, each number for 1 s, until the number "1" was finally displayed. Synchronized with this countdown, subjects made repeated tapping movements with the same finger 12 times, with each tap lasting 1 s. The fixation cross was displayed for 10 s during interblock intervals.

These results strongly indicate the experience-dependent plasticity of the somatotopic map in S1.

Compared with S1, the organizing principle, as well as the plasticity of finger representations in M1, is still unclear. It has been proposed that M1 does not follow a simple somatotopic orderly organization but has a complex structure reflecting coordinated movements of multiple fingers (Meier et al., 2008). A study on monkeys showed that intensive training of dexterous finger control results in the modification of the topological map in M1 (Nudo et al., 1996). A recent study used multi-voxel pattern analysis (MVPA) of fMRI activations in humans (Ejaz et al., 2015). MVPA allows more detailed investigations of neural representations compared with conventional univariate analysis (Haynes and Rees, 2005; Kamitani and Tong, 2005; Norman et al., 2006) and could thus be used for analyzing complex and overlapping representations of individual fingers (Diedrichsen et al., 2013; Wiestler et al., 2011), especially in M1 lacking a clear somatotopy. Their results showed that the representation of individual fingers is determined by the everyday experience of coordinated patterns of finger movements (Ejaz et al., 2015). This indicates the principle of use-dependent organization of somatotopic maps in M1. However, in addition to everyday movements in general subject populations, it is still unclear whether individual differences in finger movements in the long term might also affect such a representation of the finger map.

Here, we investigated the effect of individual training experience of finger movements on the representation of digits in the primary sensorimotor cortex. To that end, we compared participants with experience in piano training with novice subjects without such training. To eliminate a possible confounding in behavioral performance between the trained and novice groups, we employed simple visually triggered repetitive tapping movements with individual fingers. Using MVPA, we analyzed the spatial activation patterns during finger movements and tried to identify that finger which showed movement. It is known that trained musicians show a decreased activation in M1 (Jäncke et al., 2000; Krings et al., 2000) or in the higher-order motor association areas (Haslinger et al., 2004). In such cases, MVPA is most suited for analyzing the spatial activation patterns rather than the magnitude of averaged activation within ROIs. We predicted that, if prior long-term training affects the reorganization of finger representations in the sensorimotor cortex, the pattern of voxel activation could be different between the different groups, which may further result in distinct levels of classification accuracies for individual fingers.

2. Materials and methods

2.1. Participants

Participants included 40 healthy volunteers. Written informed consent was obtained from all participants in accordance with the Declaration of Helsinki. The experimental protocol was approved by the local ethics committee. Their handedness was assessed by a modified version of the Edinburgh Handedness Inventory (Oldfield, 1971) for Japanese participants (Hatta and Nakatsuka, 1975). The participants were distributed into two groups: one group consisted of 20 amateur musicians with prior experience of practicing the piano (mean experience = 17.89 years; SD = 4.16; range = 9–26) along with active current experience in playing the instrument (trained group; 8 males and 12 females; 19–28 years of age; 2 left-handed), and the second group included 20 participants with no prior experience of instrumental practice, except that acquired during school education (novice group; 8 males and 12 females; 19–32 years of age; 3 left-handed). Two sample t-tests revealed no statistically significant differences in ages between the two groups ($t(37) = 0.99$, $p = .33$, Cohen's $d = 0.33$).

Table 1
Anatomical regions, peak voxel coordinates, and t-values of observed activations.

Anatomic region	voxels	MNI coordinates			*t*-value
		x	y	z	
Right hand > Left hand					
R Cerebellum	187	15	−52	−22	16.19
L Precentral cortex	415	−36	−22	53	13.45
L Postcentral cortex		−48	−22	53	9.80
L Thalamus	13	−15	−22	8	8.01
L Putamen	17	−30	−13	2	7.54
L Rolandic operculum	10	−45	−22	23	7.07
Left hand > Right hand					
L Cerebellum	262	−18	−52	−19	19.17
R Postcentral cortex	383	36	−22	47	11.59
R Precentral cortex		36	−22	62	10.02
R Thalamus	29	15	−22	5	9.31
R Putamen	68	30	−7	−1	8.50
R Rolandic operculum	32	45	−25	20	7.49

MNI, Montreal Neurological Institute; L, left hemisphere; R, right hemisphere.

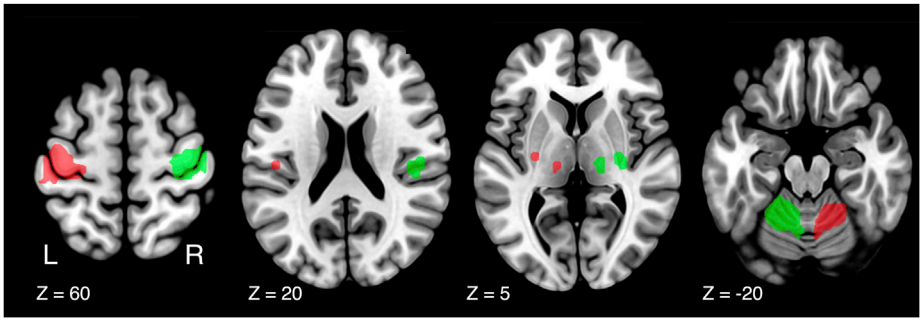

Fig. 2. Activated regions in the fMRI univariate analysis. Red: areas activated by the tapping of the right hand compared with the tapping of the left hand. Green: areas activated by the tapping of the left hand compared with that of the right hand. Activation was reported with a threshold of $p < .05$ corrected for multiple comparisons for family-wise error (FWE) with an extent threshold of 10 voxels. L, left hemisphere; R, right hemisphere. MNI coordinates of activated foci are reported in Table 1. Figures are displayed in the horizontal plane with Z denoting locations in the MNI coordinates.

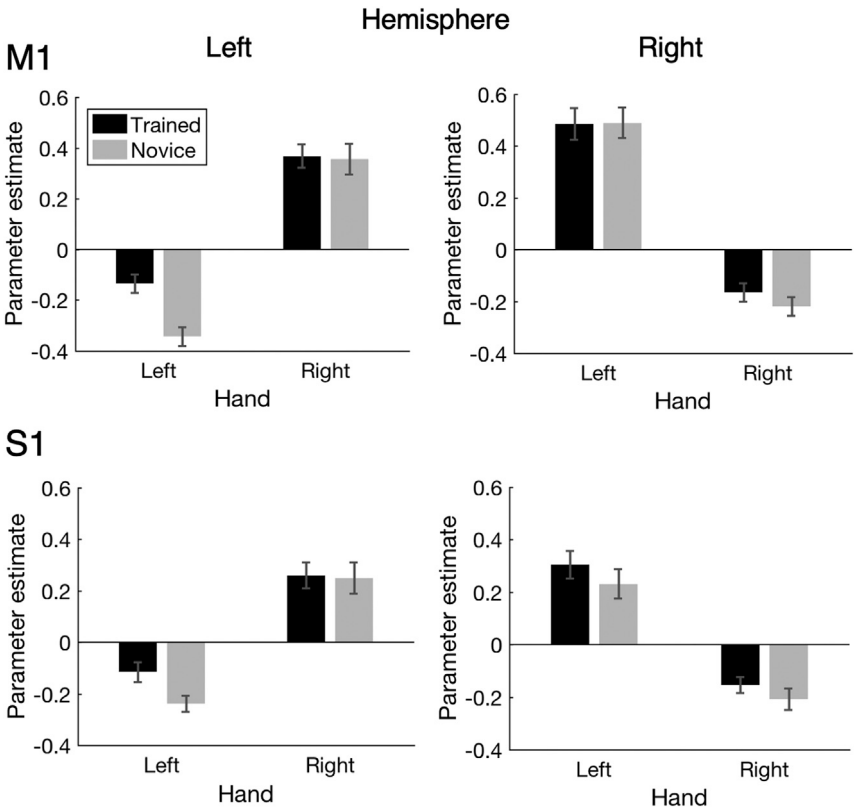

Fig. 3. The averaged activation (parameter estimates) within ROIs. The left and right panels show activations in the left and right hemispheres, respectively. Within the panel, the left and right bars represent activations by tapping using the left and right hands, respectively, for the two groups. M1, primary motor area; S1, primary somatosensory area; error bars indicate SEMs.

2.2. Task procedures

The participants performed individual finger tapping the index (D2), middle (D3), ring (D4), and little (D5) fingers following a visual cue (a single Japanese character) shown on the upper middle part of a screen, above the center fixation cross (Fig. 1). Two seconds later, the number "12" was displayed under the fixation cross and counted down for 1 s until "1" was displayed. Synchronized with the timing of this visual cue, the subjects made repeated tapping movements with the same finger 12 times, once for every second. We recorded the tapping response using an MRI-compatible response pad (Current Design, Philadelphia, USA). A fixation cross was displayed for 10 s during interblock intervals. The participants underwent a total of eight sessions (four each for the right and left hands), with each session composed of 12 blocks, and the session order was counterbalanced across participants. One session lasted approximately 5 min.

Stimuli were presented on a liquid crystal display and projected onto a custom-made viewing screen. The participants took a supine position in the scanner and viewed the screen via a mirror such that they were unable to view their hand throughout this task. The heads of the participants were immobilized with foam pads to minimize movements. The maximum amount of head movement of each participant, estimated by aligning the functional images (see below), ranging from 0.32 to 2.26 mm, with a median of 0.77 mm within a session. No statistically significant differences were observed in the maximum head movements between the trained and novice groups ($t(37) = -0.63$, $p = .53$, $d = 0.21$).

2.3. MRI acquisition

All scans were performed on a Siemens (Erlangen, Germany) 3-Tesla Prisma scanner with a 64-channel head coil at Hokkaido University. T2*-weighted echo planar imaging (EPI) was used to acquire a total of 99 scans per session, with a gradient echo EPI sequence. The first three scans within each session were discarded in order to allow for T1 equilibration. The scanning parameters were repetition time (TR), 3000 ms; echo time (TE), 30 ms; flip angle (FA), 90°; field of view (FOV), 192 × 192 mm; matrix, 94 × 94; 36 axial slices; and slice thickness, 3.0 mm with a 0.75 mm gap. T1-weighted anatomical imaging with an MP-RAGE sequence was performed using the following parameters: TR, 2300 ms; TE, 2.32 ms; FA, 8°; FOV, 256 × 256 mm; matrix, 256 × 256; 192 axial slices; and slice thickness, 1 mm without a gap.

2.4. Processing of fMRI data

Image preprocessing was performed using the SPM12 software (Wellcome Department of Cognitive Neurology, http://www.fil.ion.ucl.ac.uk/spm). All functional images were initially realigned to adjust for motion-related artifacts. Volume-based realignment was performed by co-registering images using rigid-body transformation to minimize the squared differences between volumes. The realigned images were then spatially normalized with the Montreal Neurological Institute (MNI) template based on the affine and non-linear registration of co-registered T1-weighted anatomical images (normalization procedure of SPM). They were resampled into 3-mm-cube voxels with sinc interpolation. Images were spatially smoothed using a Gaussian kernel of 6 × 6 × 6-mm full width at half-maximum. The images used for MVPA were not smoothed to avoid blurring the fine-grained information contained in the multi-voxel activity (Mur et al., 2009; but see, Kamitani and Sawahata, 2010).

Using the general linear model (GLM), the 12 blocks per session were modeled as separate 12 box-car regressors that were convolved with a canonical hemodynamic response function. Low-frequency noise was removed using a high-pass filter with a cut-off period of 128 s, and serial correlations among scans were estimated with an autoregressive model

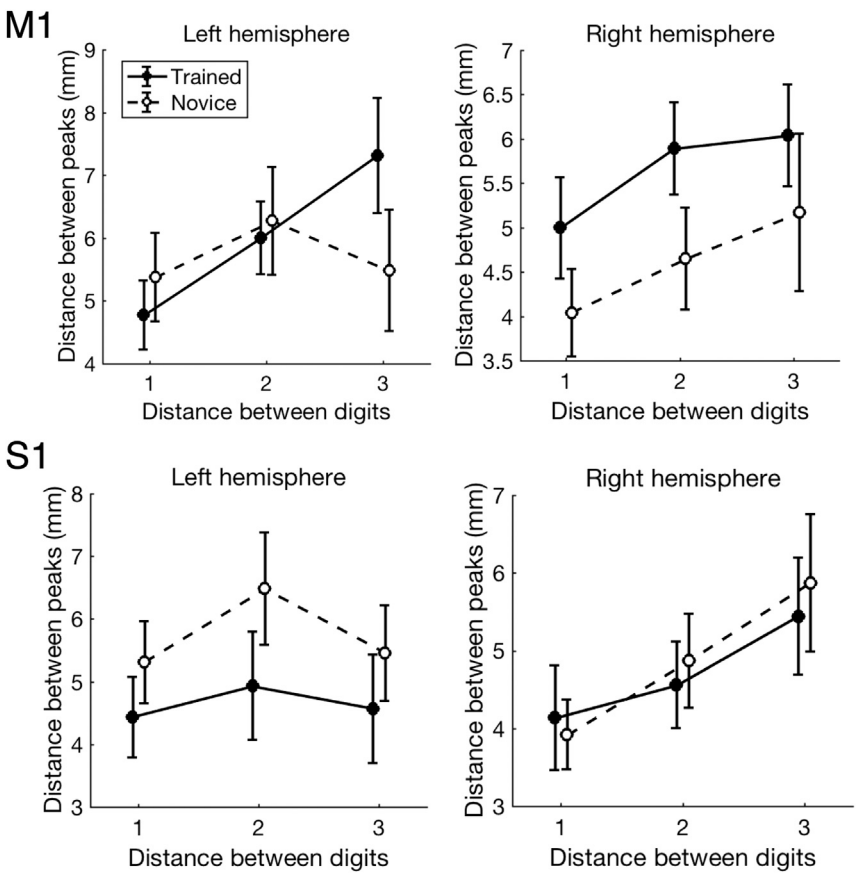

Fig. 4. The averaged peak distances (mm) between each pair of digits. Distance 1 represents neighboring pairs (e.g., D2 and D3), distance 2 represents finger pairs separated by one digit (e.g., D2 and D4), and distance 3 represents finger pairs separated by two digits (D2 and D5). Solid and dashed lines represent the trained and novice groups, respectively. The upper and lower rows represent the primary motor cortex (M1) and the primary somatosensory cortex (S1), respectively. Error bars indicate SEMs.

implemented in SPM12. This analysis yielded 12 independently estimated parameters (beta values) per session for each individual voxel. These parameter estimates were then *z*-normalized across voxels for each trial and were subsequently used as inputs to MVPA.

2.5. Definition of regions of interest (ROIs)

ROIs related to finger movement were individually defined within the sensorimotor cortex. First, Freesurfer (http:// surfer.nmr.mgh.harvard.edu/; Dale et al., 1999) was used to reconstruct the pial and white-gray matter surfaces using the T1-weighted anatomical images. Anatomical ROIs were then defined on the group average surface and projected into the individual brain based on reconstructed individual anatomical surfaces. This method ensured the precise definition of ROIs by considering individual differences in the folding structures, and has been widely used in previous studies focusing on M1 (Diedrichsen et al., 2013; Ejaz et al., 2015; Haar et al., 2017; Schellekens et al., 2018; Wiestler et al., 2011; Yokoi et al., 2018). The hand region of M1 was individually defined as the surface nodes with the highest probability for the Brodmann area (BA) 4, and was located within 2.5 cm below and above the precentral knob (Yousry et al., 1997), which were also defined on individual T1 images. S1 was similarly defined within BA 3a, 3b, 1, 2 (combined) and was 2.5 cm below and above the precentral knob. Next, finger-related functional ROIs were localized using fMRI data from another group of participants (n = 15; 11 males; 21–37 years of age; all right-handed). These subjects did not participate in the main experiment and were not questioned about prior musical training. This group was scanned while performing the same tapping task as the participants of the main experiment. We analyzed the areas that were significantly activated during tapping with the left and right hands compared with activation during the rest period. Contrast image results from each subject, which were generated using a fixed-effects model, were analyzed using a random-effects model and one-sample *t*-test. Activities were thresholded at $p < .05$, uncorrected at the voxel-level, in the hemisphere contralateral to the hand and were then inclusively masked with the anatomical ROIs. The cerebellum, putamen, and thalamus were also included in the ROIs. These ROIs were both functionally and anatomically defined in the same manner for the M1 and S1, except those of the cerebellum that were defined in the hemisphere ipsilateral to the hand.

2.6. fMRI mass-univariate analysis

We used the conventional mass-univariate analysis of individual voxels to reveal activated areas for finger tapping. We analyzed areas for the left and right hands that were significantly activated during tapping compared with activation during the rest period. Contrast images of each participant, generated using a fixed-effects model, were analyzed using a random-effects model of a one-sample *t*-test. Activation was reported with a threshold of $p < .05$ corrected for multiple comparisons for a family-wise error (FWE) with an extent threshold of 10 voxels.

2.7. Multi-voxel pattern classification

We used the multivariate pattern analysis of fMRI to identify and classify the finger being moved by the subjects. The classification was performed with a multi-class classifier based on a linear support vector machine (SVM) implemented in LIBSVM (http://www.csie.ntu.edu.tw/~cjlin/libsvm/) with default parameters (a fixed regularization parameter C = 1). Multi-class classification, implemented in LIBSVM, was used to classify the four digits using the "one-against-one"

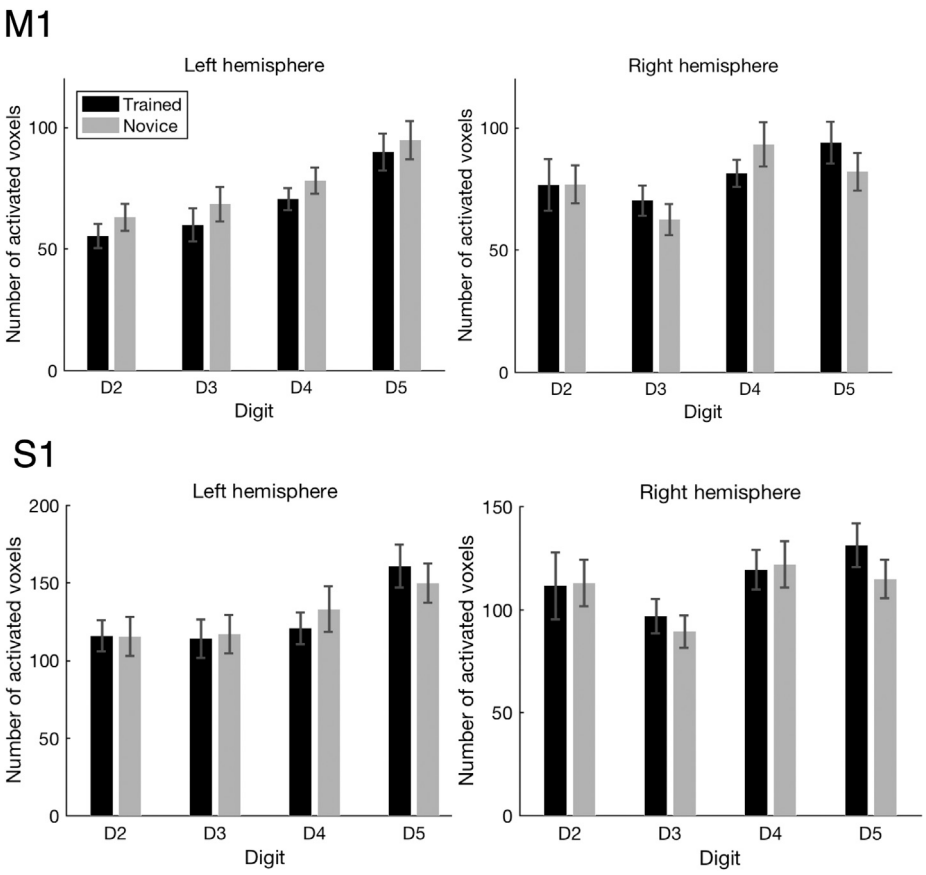

Fig. 5. The average number of activated voxels for each digit in each hemisphere contralateral to the hand used for tapping, for the trained and novice groups. D2, D3, D4, and D5 represent the index, middle, ring, and little fingers, respectively. The left and right graphs represent the activated voxels for contralateral finger movements in the left and right hemispheres, respectively. Error bars indicate SEMs.

method, wherein all pairwise classifiers among the digits were conducted, and each output was then compared to produce the label with maximal probability. Parameter estimates (beta values) for each trial of voxels within ROIs were used as inputs to the classifier. The averaged classification accuracy was estimated with a four-fold "leave-one-out" cross-validation. This was based on four sessions per subject, in which three sessions were used as a training and one remaining session was used as test data. A one-sample *t*-test was used to determine whether the observed decoding accuracy was significantly higher than chance (25.0%) with inter-subject difference treated as a random factor.

2.8. Representational similarity analysis

In addition to the classification analysis, we conducted a representational similarity analysis (RSA) (Kriegeskorte et al., 2008) in order to compare the similarity of spatial activation patterns for each pair of fingers. Similar to the classification analysis, the parameter estimates (beta values) of voxels within ROIs were used as inputs to estimate the representational dissimilarity matrix (RDM) among different digits. Dissimilarity was measured with cross-validated Mahalanobis distance (Ejaz et al., 2015), which presents reliable dissimilarity metrics for RSA (Walther et al., 2016). We applied the same fold structure as that of the "leave-one-session-out" in the classification analysis. One session was assigned to one dataset, and the remaining three sessions were assigned to the other dataset. The distance estimates were then averaged across folds. To ensure invertibility and stability, the voxel-by-voxel noise covariance matrix was separately estimated within one dataset using an optimal-shrinkage algorithm (Ledoit and Wolf, 2003). We then compared the off-diagonal elements of RDM, which represent the dissimilarity of activation patterns between different digits between the trained and novice groups.

3. Results

3.1. Behavioral analysis

We defined a correct trial as that trial when the subject tapped the instructed finger between 9 and 15 times out of 12 times, which was visually cued per block. One participant within the trained group was excluded from further analysis because of poor performance. Almost all of the remaining subjects performed the finger-tapping task correctly. Out of the 96 trials per subject, the mean numbers of erroneous trials were 0.42 and 0.65 for the trained and novice groups, respectively. The results of the Mann–Whitney *U* test indicated that the number of error trials was not significantly different between the two groups ($U = 149$, $p = .19$). We also compared the tapping interval per block with the right and left hands collapsed over four fingers between the two groups. For the right hand, the average tapping intervals (SD) were 976.81 (88.49) ms and 973.90 (93.21) ms in the trained and novice groups, respectively. For the left hand, the average tapping intervals were 976.29 (89.45) ms and 972.62 (95.29) ms in the trained and novice groups, respectively. The two-way analysis of variance (ANOVA) with the hands (right and left) as a within-subject factor and the groups (trained and novice) as a between-subject factor revealed no significantly main effects nor interactions in the average and SD of intervals ($Fs(1, 37) < 0.93$, $ps > .34$, $\eta_p^2 s < 0.03$).

3.2. fMRI mass-univariate analysis

We analyzed the activated regions of the brain using conventional

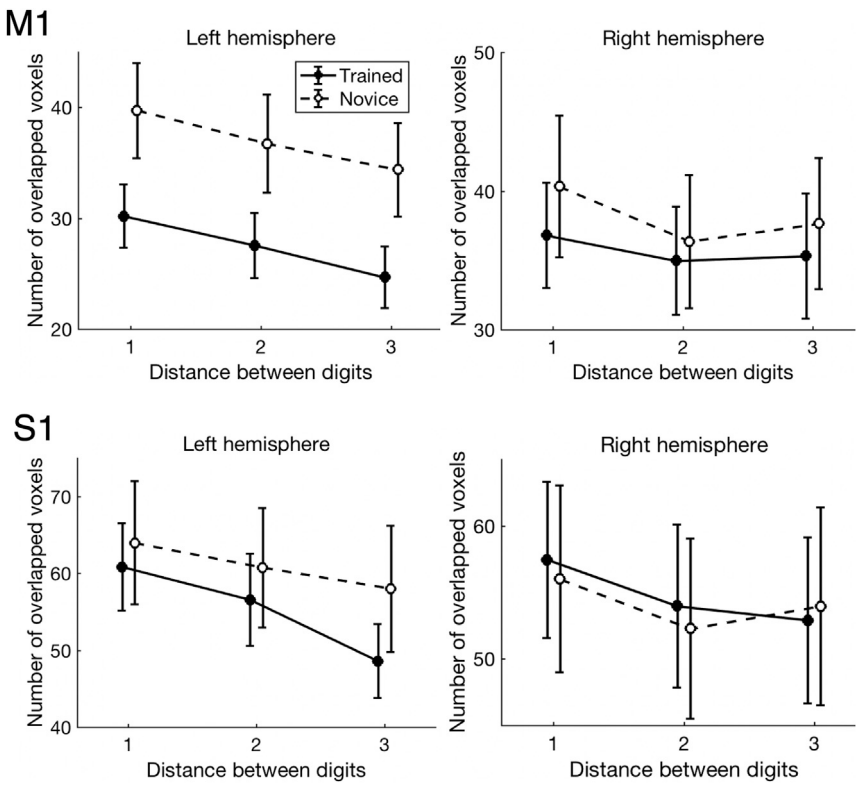

Fig. 6. The average number of overlapped voxels between each pair of digits according to their distances: distance 1 represents neighboring pairs (e.g., D2 and D3), distance 2 represents the consecutive next finger pairs (e.g., D2 and D4), and distance 3 represents the next three finger pairs (D2 and D5). The left and right graphs represent the activated voxels for contralateral finger movements in the left and right hemispheres, respectively. Error bars indicate SEMs.

univariate analysis of single voxels and the regions that were significantly activated during tapping by comparing the right and left hands, collapsed across the digits. This comparison revealed the activations largely in the primary motor and somatosensory cortex contralateral to the hand and the ipsilateral cerebellum, together with small clusters in the putamen, thalamus, and rolandic operculum in the contralateral hemisphere (Fig. 2 and Table 1). Next, we compared the identical contrasts (right vs. left hand) between the trained and novice groups. This revealed no significantly activated areas even at a higher liberal uncorrected threshold of $p < .001$ and an extent threshold of 10 voxels.

Next, ROI analysis was performed to compare the averaged parameter estimates (beta values) between the hands within the two groups. Two-way ANOVA was conducted with hands (right and left) as a within-subject factor and groups (trained and novice) as a between-subject factor (Fig. 3). In the case of both left and right M1, a significant main effect was observed between the two hands (left hemisphere, $F(1, 37) = 198.13$; right hemisphere, $F(1, 37) = 154.17$; both $p < .001$, η_p^2s > 0.80), indicating greater activation during use of the contralateral hand compared with the ipsilateral hand. A significant interaction was observed only in the left M1 ($F(1, 37) = 5.38$; $p < .05$, $\eta_p^2 = 0.13$) with a significant simple main effect between groups in the left hand ($p < .05$). In S1, a significant main effect was observed between the use of the two hands (left hemisphere, $F(1, 37) = 116.67$; right hemisphere, $F(1, 37) = 91.31$; $ps < .001$, η_p^2s > 0.71), indicating greater activation during the use of the contralateral hand compared with the ipsilateral hand. No significant effect between the groups or interactions was observed ($ps > .05$). Similarly, we found a significant main effect between hands ($ps < .05$, η_p^2s > 0.40) but no significant main effect between groups or interactions in the cerebellum, putamen, and thalamus in both hemispheres ($ps > .05$; Supplementary Fig. 1).

Following these observations, we analyzed the extent of activation caused by tapping individual fingers separately. The activations that occurred within the primary sensorimotor cortex (M1/S1) during the tapping of each digit were thresholded at $p < .001$, uncorrected at the voxel level, for individual subjects. The activated clusters showed separate locations that largely overlapped between digits (Supplementary Fig. 2). In general, the peak coordinates of activations showed orderly locations for individual digits; D2 activation was located more ventrally than that of D5 (Supplementary Fig. 3). Subsequently, we analyzed the distance (mm) between the peak coordinates of activation between digits. These digit-distances were averaged: distance 1 represents neighboring pairs (e.g., D2 and D3), distance 2 represents finger pairs separated by one digit (e.g., D2 and D4), and distance 3 represents finger pairs separated by two digits (D2 and D5) (Fig. 4). A two-way ANOVA with the three digit-distances as a within-subject factor and groups as a between-subject factor was conducted. In M1, a significant main effect of digit-distance (left hemisphere, $F(2, 74) = 3.70$, $p < .05$, $\eta_p^2 = 0.09$; right hemisphere, $F(2, 74) = 3.24$, $p < .05$, $\eta_p^2 = 0.08$) was found, which indicates that the distance between activation peaks for the pairs of near digits is closer than those for distant digit pairs, with significant interaction in the left hemisphere ($F(2, 74) = 3.29$, $p < .05$, $\eta_p^2 = 0.08$). S1 showed significant effect of digit-distance in the right hemispheres ($F(2, 74) = 5.96$, $p < .005$, $\eta_p^2 = 0.14$), but not in the left hemisphere ($p > .05$), without any significant interactions. Importantly, there were no significant effects for groups for both M1 and S1 ($ps > .05$).

The number of activated voxels for individual fingers were tested using a two-way ANOVA using digits (D2, D3, D4, and D5) as a within-subject factor and groups (trained and novice) as a between-subject factor. The analysis was performed with minimal thresholding of activations ($p < .05$ uncorrected at the voxel level) and without spatial smoothing. It revealed a significant main effect of digits for M1 and S1 in both hemispheres ($Fs(3, 111) > 6.33$, $ps < .001$, η_p^2s > 0.14), with no statistically significant effects for groups or interactions ($ps > .05$; Fig. 5). In addition, the number of overlapped voxels between neighboring digits

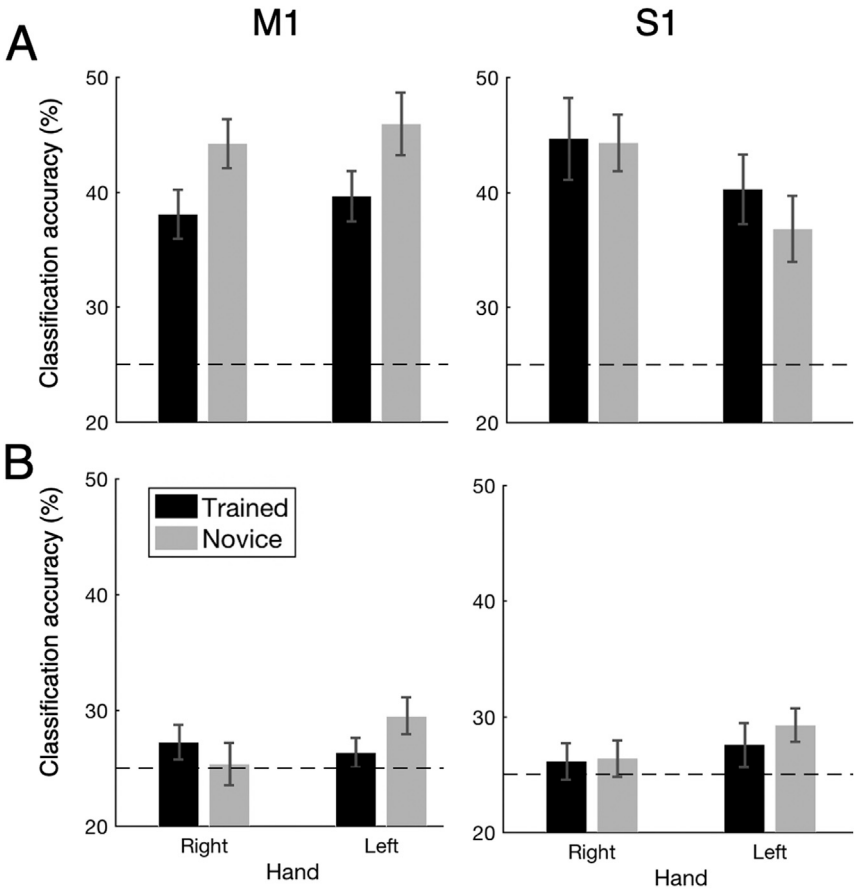

Fig. 7. The averaged classification accuracies for finger tapping with the right and left hands. The ROI contralateral to the hand was selected (e.g., the activity of ROI in the left hemisphere is used for the classification of the right hand) in the upper row (A), while the hemisphere ipsilateral to the hand is shown in the lower row (B). M1, primary motor area; S1, primary somatosensory area. Error bars indicate SEMs. Dotted lines indicate chance level (25%).

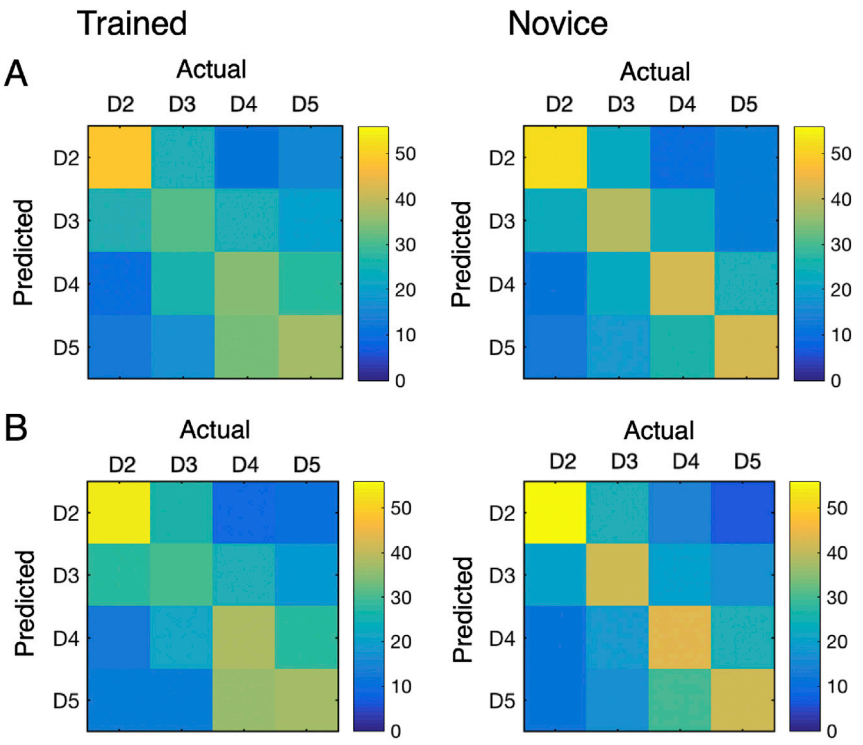

Fig. 8. The confusion matrix of the classification results between the digits of the trained group (left column) and the novice group (right column). The upper (A) and lower (B) rows represent the results obtained for the left and right hemispheres, respectively. Each cell represents the percentage ratio (%) of correct classifications determined in each experiment, with the rows and columns representing the predicted and the actual digits, respectively. The diagonal elements represent the classification accuracy (%) for individual digits. D2, D3, D4, and D5 represent the index, middle, ring, and little fingers, respectively.

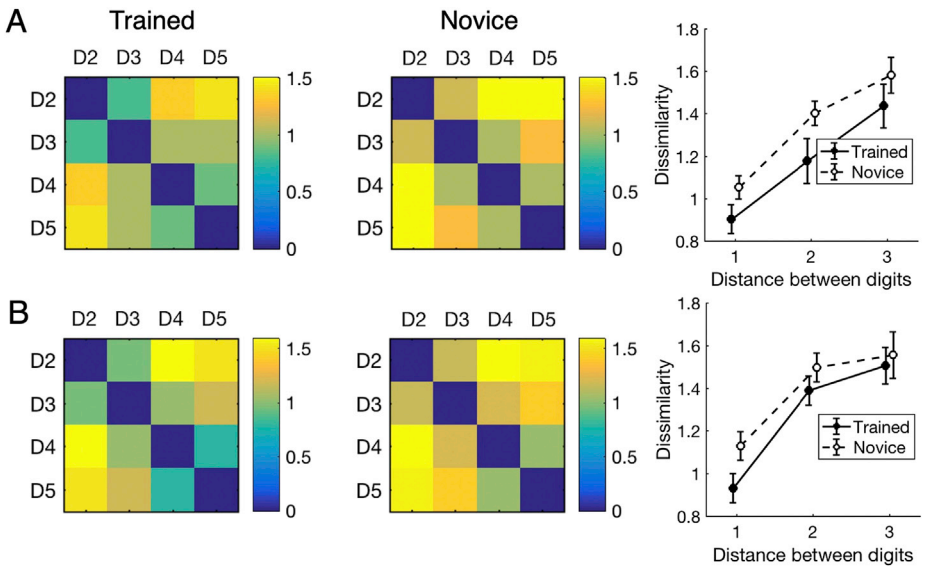

Fig. 9. Representational similarity analysis (RSA) in the primary motor cortex (M1) of the hemisphere contralateral to the hand used for tapping. Figures in the left and middle columns show the representational dissimilarity matrix (RDM) for each digit pair of the trained and novice groups, respectively. The upper (A) and lower (B) rows represent the results obtained for the left and right hemispheres, respectively. D2, D3, D4, and D5 represent the index, middle, ring, and little fingers, respectively. Figures in the right column show an averaged dissimilarity according to their distances: distance 1 represents neighboring pairs (e.g., D2 and D3), distance 2 represents finger pairs separated by one digit (e.g., D2 and D4), and distance 3 represents finger pairs separated by two digits (D2 and D5). Solid and dashed lines represent the trained and novice groups, respectively.

was tested with two-way ANOVA with digit-distance (1, 2, and 3) and groups (trained and novice). It showed a main effect of digit-distance for M1 and S1 in both hemispheres ($Fs(2, 74) > 3.16$, $ps < .05$, $\eta_p^2 s > 0.07$) with no statistically significant differences between groups nor interaction ($ps > .05$; Fig. 6).

3.3. Multi-voxel classification analysis

We conducted MVPA to classify the finger being moved by the subjects using the activities of each ROI contralateral to the hand (e.g., the activity in the left hemisphere was used for classification of the right hand; Fig. 7A). In M1, significantly higher-than-chance classification accuracies were observed in both groups with both hands: right hand (trained group, $t(18) = 6.15$, $d = 1.45$; novice group, $t(19) = 9.10$, $d = 2.08$, $ps < .001$) and left hand (trained group, $t(18) = 6.74$, $d = 1.59$; novice group, $t(19) = 7.66$, $d = 1.76$, $ps < .001$). In S1, we also found significantly higher-than-chance classification accuracies in both groups using both hands: right hand (trained group, $t(18) = 5.52$, $d = 1.30$; novice group, $t(19) = 7.87$, $d = 1.81$, $ps < .001$) and left hand (trained group, $t(18) = 5.05$, $d = 1.19$; novice group, $t(19) = 4.11$, $d = 0.94$, $ps < .001$). A two-way ANOVA was then conducted with hands (right and left) as a within-subject factor and groups (trained and novice) as a between-subject factor. In M1, we found significant effects of the group ($F(1, 37) = 9.66$, $p < .005$, $\eta_p^2 = 0.21$), indicating a lower accuracy within the trained group as compared with the novice group and no significant main effects of the hand and the interaction ($Fs(1, 37) < 0.40$, $ps > .53$, $\eta_p^2 s < 0.02$). In S1, we observed a significant main effect of hands ($F(1, 37) = 4.81$, $p < .05$, $\eta_p^2 = 0.12$), indicating a lower accuracy for the left hand than for right, without a significant main effect for groups or interactions ($Fs(1, 37) < 0.35$, $ps > .56$, $\eta_p^2 s < 0.01$).

We also performed MVPA to classify the finger being moved using the activities detected in ROIs ipsilateral to the hand (Fig. 7B). The accuracies in classification were lower than those using activities from the contralateral hemispheres and were around chance-level. A two-way ANOVA with hands and groups showed no significant main effect and interaction ($ps > .05$). For the remaining ROIs, the cerebellum showed significantly above-chance accuracy in the ipsilateral hemisphere to the hand used under any conditions ($ps < .05$, $ds > 0.45$), while the putamen and thalamus showed no significantly above-chance accuracy for either hemisphere ($ps > .05$; Supplementary Fig. 4). Furthermore, there was no significant main effect of group or interactions in these ROIs ($ps > .05$).

The confusion matrix of the M1 was calculated based on the classification results (Fig. 8). Each cell represents the percentage ratio of correct classifications determined in each experiment, with the rows and columns representing the predicted and actual digits, respectively. The diagonal elements represent the classification accuracy (%) for individual digits. The matrix shows that in general the adjacent fingers tended to be misclassified compared with the distal fingers.

We further conducted a correlation analysis between the classification accuracy of the contralateral hemisphere and the length of the training period of each subject in the trained group. We found no significant correlation coefficients in M1 ($|r| < 0.18$, $p > .45$) and in S1 ($|r| < 0.20$, $p > .42$). We also analyzed the correlation coefficient between the classification accuracies and the age of commencement of training (mean age = 5.3; SD = 2.9; range = 2–12) and observed no significant correlations in both M1 and S1 ($ps > .10$).

3.4. Representational similarity analysis

The RSA was used to investigate similarity in activation patterns of M1 between each pair of digits. The estimated RDM showed that movements within the pairs of near digits (e.g., D2 and D3) produced highly similar activation patterns compared with those with distant digit pairs (D2 and D5) for both the right and left hands (Fig. 9, left and middle column). We then compared the dissimilarity of activation patterns between the trained and novice groups, represented in the off-diagonal elements of RDM. Dissimilarities were averaged according to their digit-distances: distance 1 (e.g., D2 and D3), distance 2 (e.g., D2 and D4), and distance 3 (D2 and D5; Fig. 9, right column). A two-way ANOVA was conducted with the distance between the digits (1, 2, and 3) as a within-subject factor and the groups (trained and novice) as a between-subject factor. A significant effect of distance between the digits was found in both the right ($F(2, 74) = 69.45$, $p < .001$, $\eta_p^2 = 0.65$) and left hands ($F(2, 74) = 41.64$, $p < .001$, $\eta_p^2 = 0.53$). The main effects of group were marginally significant for the right hand ($F(1, 37) = 2.90$, $p = .09$, $\eta_p^2 = 0.07$) but not for the left hand ($F(1, 37) = 1.74$, $p = .20$, $\eta_p^2 = 0.04$) without any significant interaction. The RDM of the hemisphere ipsilateral to the hand was also analyzed and this revealed no clear structure (finger movements within near digit pairs generate similar activity pattern) compared with the contralateral side (Supplementary Fig. 5).

4. Discussion

This study investigated the effect of long-term training on the neural

representation of individual finger movements within the primary sensorimotor cortices by comparing a group of participants with prior experience and training in playing the piano with a novice group with no such training. Our results confirmed the absence of significant differences in behavioral measures, including tapping accuracy and average tapping interval as well as its variability (SD) between the groups. We found that the classification accuracy for individual fingers was significantly lower in M1 within the trained group compared with that in the novice group. No significant differences were observed in averaged signal changes and the number of activated voxels for individual digits, or the extent of overlap between adjacent digits. Our results indicate the modulation of neural representations of individual finger movements of M1 due to long-term prior piano training.

Our mass-univariate analysis revealed that the activated clusters for individual digits showed separation in location, but were highly overlapped between digits. This tendency is generally consistent with a previous fMRI study showing large overlaps in activation between digits (Ejaz et al., 2015). Our results also showed that the number of activated voxels for individual digits and the extent of overlap between digits were not significantly different between the trained and novice groups. A previous fMRI study showed that the extent of activations was enlarged for movements of learned finger sequences compared with unlearned ones (Karni et al., 1995). While the study by Karni and colleagues used pre-specified sequences of finger movements, we employed simple repetitive tapping with an individual finger, which produced no significant differences in the size of activated clusters between the trained and novice groups. Trained musicians are also known to show decreased activation in motor-related areas including the M1 (Jäncke et al., 2000; Krings et al., 2000). These previous studies employed complex bimanual finger tapping or pre-specified sequences of finger movements at self-paced speeds. Their findings indicate neural efficacy in trained musicians, as they produce less activation than control subjects in motor-related areas. In contrast, the current study used simple individual finger-tapping movements with an external cue at fixed speeds, which avoided confounding in behavioral performance as well as general task-related difficulties between the trained and novice groups. The discrepancy between previous studies and the present results regarding the amplitude or extent of activations may be due to differences in the complexity of the finger movement task employed.

We found that the classification accuracies of the novice group were generally higher in M1 than those in S1 (Fig. 7). While caution is required to compare accuracies between different ROIs, this result may contradict with the finding that the specificity of individual digit representations is more somatotopically separated in S1 (see Roux et al., 2018) than that those in M1 (Meier et al., 2008). One possible reason is that the current study used an active tapping task, whereas previous studies investigating somatotopy in S1 mostly used passive tactile stimulation. Self-produced movement is known to induce sensory attenuation of tactile sensation (Blakemore et al., 2000, 1999, 1998). We found that average signal increases during tapping were generally higher in M1 than in S1 (Fig. 3), which is in agreement with the account of sensory attenuation.

The results from the RSA showed that finger movements within near digit pairs (e.g., index and middle fingers) generate highly similar activation patterns when compared with those with distant digit pairs (e.g., index and ring fingers). This finding is consistent with that reported in a previous study (Ejaz et al., 2015). The dissimilarity between digits in RDM was higher in the novice group than in the trained group at a marginally significant level. This result is consistent with significantly higher classification accuracy in the novice group than in the trained group.

A previous study with monkeys had reported use-dependent plasticity of the topological map in M1 upon the training of skilled digit manipulations (Nudo et al., 1996). Another study indicated that the M1 neuronal activity reflects an acquired motor skill that requires a skilled sequential movement (Matsuzaka et al., 2007). A human study with structural MRI or voxel-based morphometry (VBM) reported an increased hand region or gray matter volume of the sensorimotor cortex in professional musicians (Bangert and Schlaug, 2006; Gaser and Schlaug, 2003). Together, these studies indicate the importance of motor skill learning on the neural representation of M1. A recent study with MVPA proposed the hand-usage model to explain the representation of digits in M1, indicating that the neural representation of digits reflects the coordinated pattern of everyday movements (Ejaz et al., 2015). The results of our study are consistent with earlier reports, and these results were further able to demonstrate the effect of individual daily experiences on the somatotopic representation of fingers in M1.

We found a significantly lower classification accuracy in the trained group compared with the novice group, indicating a higher similarity between the neural representations of individual fingers in the trained subjects. This finding may appear to be counterintuitive considering that dexterous control of finger movements in musical training could cause expansion or differentiation of individual finger representations (e.g., Elbert et al., 1995) and higher classification accuracy of digits. Instead, we consider that a lower accuracy in trained participants arose because of the coordinated use of multiple fingers during piano training. Playing the piano requires the simultaneous and highly coordinated use of multiple fingers, which may lead to migration of individual finger representations in M1. It is known that M1 does not follow a simple somatotopic orderly organization but has a structure that reflects coordinated movements of multiple fingers (Meier et al., 2008). A study with monkeys showed that intensive training of dexterous finger control results in the modification of the topological map in M1 (Nudo et al., 1996). These studies are consistent with the proposal that attributes M1 as a repertoire of movements with the coordinated use of effectors, rather than an effector-dependent somatotopic map (Graziano and Aflalo, 2007). A recent study which used transcranial magnetic stimulation (TMS) showed that an implicit learning of sequential finger movements induces a reorganization of the cortico-spinal system, including M1 (Hirano et al., 2018). Consistent with these previous findings, our results indicate that the long-term training of coordinated movement of multiple fingers results in the cortical reorganization of digit representations in M1.

It is well accepted that focal hand dystonia or writer's cramp, which is observed in music players, is caused by the reduced inter-digit separation or de-differentiation of individual fingers in S1 (Bara-Jimenez et al., 1998; Butterworth et al., 2003; Catalan et al., 2012; Elbert et al., 1998; Nelson et al., 2009; Weise et al., 2012). By combining TMS with hand muscle vibrations, it was shown that not only dystonic patients but also healthy musicians exhibit expanded somatotopic representations of fingers in S1 (Rosenkranz et al., 2005). On the basis of this finding, the aforementioned authors proposed that focal dystonia represents a progression in the reorganization observed in normal musical players. Contrastingly, our current results did not reveal any significant difference in classification accuracies of S1 between the trained and novice groups. This discrepancy could be attributed to the fact that previous studies mainly used vibration or tactile stimulation of digits, whereas the current study employed pressing of buttons with individual fingers. This may have induced less intensive tactile inputs in S1. The other difference is that previous studies used professional musicians as subjects, whereas our study employed amateur players, which inherently results in differences in the amount of musical training. Although a further study using tactile stimulation may be needed to reveal somatotopic representation in S1, our current results indicate that finger representation in M1 is affected by individual differences in finger movements by long-term musical training in addition to routine movements.

One limitation of the current study is a lack of detailed localization of the primary sensorimotor cortex using the T1-weighted anatomical image. Recent studies have used an ultra-high-field 7T scanner or a customized 3T scanner with high spatial resolution (<1 mm) to parcellate the cortex of individual subjects based on myeloarchitecture (Geyer et al., 2011; Glasser et al., 2016; Tardif et al., 2016; Waehnert et al., 2016). These studies indicate that the T1-weighted structural image with higher spatial resolution enables the detection of densely myelinated

areas around the central sulcus. We analyzed the voxel signal intensities within BA 4p and 3a from individual anatomical T1 images and found that the distributions largely overlapped (Supplementary Fig. 6). Thus, we considered that it is difficult to detect the precise boundary of the primary motor cortex using the voxel intensities in the current data. In addition, a recent 7T MRI study proposed Gaussian population receptive field analyses (Schellekens et al., 2018). This method aims to analyze the gradients of individual digit repesentaions using a BOLD time-series in which subjects sequentially move their fingers from thumb to little finger or vice versa. These advancements in MRI mesurements and analysis methods should enable the precise localization and identification of individual finger representations in M1 and S1 for future studies. The second limitation is that our current study lacks correspondence between the behavioral data and MVPA results. We consider that the analysis of co-occurring patterns of multiple finger movements for piano-players may be difficult, as they are dependent on each musical score as well as individual experience. However, it should be noted that the confusion matrix of the decoding results (Fig. 8) indicates that the ring digit (D4) and little digit (D5) were misclassified more often compared with other pairs of digits, particularly in the trained group. Indeed, focal hand dystonic is reported to occur frequently between D4 and D5 in pianists (Newmark and Hochberg, 1987), which is relevant to our decoding results. Further study is needed to reveal the behavioral correspondence between finger representation and individual experience.

In summary, using multivariate analysis of fMRI activities, we found that neural representations of individual finger movements have a relationship with the long-term training of finger movements associated with playing the piano. Our finding indicates the importance of use-dependent plasticity or experience on the reorganization of the cortical representation in M1.

Acknowledgments

This work was supported by JSPS KAKENHI Grant Numbers 16K12440 & 17H04683 to K.O. The authors would like to thank Drs. Junichi Abe, Mayumi Adachi, & Satoshi Hirose for helpful comments, Dr. Iwao Yoshino for subject recruiting, and Dr. Ritsuko Nabata, Zhengfei Hu, & Huixiang Yang for technical assistance.

Appendix A. Supplementary data

Supplementary data to this article can be found online at https://doi.org/10.1016/j.neuroimage.2019.116051.

References

Allard, T., Clark, S.A., Jenkins, W.M., Merzenich, M.M., 1991. Reorganization of somatosensory area 3b representations in adult owl monkeys after digital syndactyly. J. Neurophysiol. 66, 1048–1058.

Bangert, M., Schlaug, G., 2006. Specialization of the specialized in features of external human brain morphology. Eur. J. Neurosci. 24, 1832–1834. https://doi.org/10.1111/j.1460-9568.2006.05031.x.

Bara-Jimenez, W., Catalan, M.J., Hallett, M., Gerloff, C., 1998. Abnormal somatosensory homunculus in dystonia of the hand. Ann. Neurol. 44, 828–831. https://doi.org/10.1002/ana.410440520.

Baumgartner, C., Doppelbauer, A., Deecke, L., Barth, D.S., Zeitlhofer, J., Lindinger, G., Sutherling, W.W., 1991. Neuromagnetic investigation of somatotopy of human hand somatosensory cortex. Exp. Brain Res. 87, 641–648.

Beisteiner, R., Windischberger, C., Lanzenberger, R., Edward, V., Cunnington, R., Erdler, M., Gartus, A., Streibl, B., Moser, E., Deecke, L., 2001. Finger somatotopy in human motor cortex. Neuroimage 13, 1016–1026. https://doi.org/10.1006/nimg.2000.0737.

Blakemore, S.J., Frith, C.D., Wolpert, D.M., 1999. Spatio-temporal prediction modulates the perception of self-produced stimuli. J. Cogn. Neurosci. 11, 551–559.

Blakemore, S.J., Wolpert, D., Frith, C., 2000. Why can't you tickle yourself? Neuroreport 11, R11–R16. https://doi.org/10.1097/00001756-200008030-00002.

Blakemore, S.J., Wolpert, D.M., Frith, C.D., 1998. Central cancellation of self-produced tickle sensation. Nat. Neurosci. 1, 635–640. https://doi.org/10.1038/2870.

Braun, C., Wilms, A., Schweizer, R., Godde, B., Preissl, H., Birbaumer, N., 2000. Activity patterns of human somatosensory cortex adapt dynamically to stimulus properties. Neuroreport 11, 2977–2980.

Butterworth, S., Francis, S., Kelly, E., McGlone, F., Bowtell, R., Sawle, G.V., 2003. Abnormal cortical sensory activation in dystonia: an fMRI study. Mov. Disord. 18, 673–682. https://doi.org/10.1002/mds.10416.

Catalan, M.J., Ishii, K., Bara-Jimenez, W., Hallett, M., 2012. Reorganization of the human somatosensory cortex in hand dystonia. J. Mov. Disord. 5, 5–8. https://doi.org/10.14802/jmd.12002.

Dale, A.M., Fischl, B., Sereno, M.I., 1999. Cortical surface-based analysis: I. Segmentation and surface reconstruction. Neuroimage 9, 179–194. https://doi.org/10.1006/NIMG.1998.0395.

Dechent, P., Frahm, J., 2003. Functional somatotopy of finger representations in human primary motor cortex. Hum. Brain Mapp. 18, 272–283. https://doi.org/10.1002/hbm.10084.

Diedrichsen, J., Wiestler, T., Krakauer, J.W., 2013. Two distinct ipsilateral cortical representations for individuated finger movements. Cerebr. Cortex 23, 1362–1377. https://doi.org/10.1093/cercor/bhs120.

Ejaz, N., Hamada, M., Diedrichsen, J., 2015. Hand use predicts the structure of representations in sensorimotor cortex. Nat. Neurosci. 18, 1034–1040. https://doi.org/10.1038/nn.4038.

Elbert, T., Candia, V., Altenmüller, E., Rau, H., Sterr, A., Rockstroh, B., Pantev, C., Taub, E., 1998. Alteration of digital representations in somatosensory cortex in focal hand dystonia. Neuroreport 9, 3571–3575. https://doi.org/10.1097/00001756-199811160-00006.

Elbert, T., Pantev, C., Wienbruch, C., Rockstroh, B., Taub, E., 1995. Increased cortical representation of the fingers of the left hand in string players. Science 270 (80-), 305–307. https://doi.org/10.1126/science.270.5234.305.

Gaser, C., Schlaug, G., 2003. Brain structures differ between musicians and non-musicians. J. Neurosci. 23, 9240–9245 [pii]. https://doi.org/10.1523/JNEUROSCI.23-27-09240.2003.

Geyer, S., Weiss, M., Reimann, K., Lohmann, G., Turner, R., 2011. Microstructural parcellation of the human cerebral cortex – from Brodmann's post-mortem map to in vivo mapping with high-field magnetic resonance imaging. Front. Hum. Neurosci. 5, 19. https://doi.org/10.3389/fnhum.2011.00019.

Glasser, M.F., Coalson, T.S., Robinson, E.C., Hacker, C.D., Harwell, J., Yacoub, E., Ugurbil, K., Andersson, J., Beckmann, C.F., Jenkinson, M., Smith, S.M., Van Essen, D.C., 2016. A multi-modal parcellation of human cerebral cortex. Nature 536, 171–178. https://doi.org/10.1038/nature18933.

Graziano, M.S.A., Aflalo, T.N., 2007. Mapping behavioral repertoire onto the cortex. Neuron 56, 239–251. https://doi.org/10.1016/j.neuron.2007.09.013.

Haar, S., Dinstein, I., Shelef, I., Donchin, O., 2017. Effector-invariant movement encoding in the human motor system. J. Neurosci. 37, 9054–9063. https://doi.org/10.1523/JNEUROSCI.1663-17.2017.

Haslinger, B., Erhard, P., Altenmüller, E., Hennenlotter, A., Schwaiger, M., Gräfin von Einsiedel, H., Rummeny, E., Conrad, B., Ceballos-Baumann, A.O., 2004. Reduced recruitment of motor association areas during bimanual coordination in concert pianists. Hum. Brain Mapp. 22, 206–215. https://doi.org/10.1002/hbm.20028.

Hatta, T., Nakatsuka, Z., 1975. Handedness inventory. In: Papers on Celebrating 63rd Birthday of Prof. Ohnishi. Osaka City University, pp. 224–245.

Haynes, J.D., Rees, G., 2005. Predicting the orientation of invisible stimuli from activity in human primary visual cortex. Nat. Neurosci. 8, 686–691. https://doi.org/10.1038/nn1445.

Hirano, M., Kubota, S., Furuya, S., Koizume, Y., Tanaka, S., Funase, K., 2018. Acquisition of skilled finger movements is accompanied by reorganization of the corticospinal system. J. Neurophysiol. 119, 573–584. https://doi.org/10.1152/jn.00667.2017.

Indovina, I., Sanes, J.N., 2001. On somatotopic representation centers for finger movements in human primary motor cortex and supplementary motor area. Neuroimage 13, 1027–1034. https://doi.org/10.1006/nimg.2001.0776.

Jäncke, L., Shah, N., Peters, M., 2000. Cortical activations in primary and secondary motor areas for complex bimanual movements in professional pianists. Cogn. Brain Res. 10, 177–183. https://doi.org/10.1016/S0926-6410(00)00028-8.

Jenkins, W.M., Merzenich, M.M., Ochs, M.T., Allard, T., Guic-Robles, E., 1990. Functional reorganization of primary somatosensory cortex in adult owl monkeys after behaviorally controlled tactile stimulation. J. Neurophysiol. 63, 82–104.

Kamitani, Y., Sawahata, Y., 2010. Spatial smoothing hurts localization but not information: pitfalls for brain mappers. Neuroimage 49, 1949–1952. https://doi.org/10.1016/j.neuroimage.2009.06.040.

Kamitani, Y., Tong, F., 2005. Decoding the visual and subjective contents of the human brain. Nat. Neurosci. 8, 679–685. https://doi.org/10.1038/nn1444.

Karni, A., Meyer, G., Jezzard, P., Adams, M.M., Turner, R., Ungerleider, L.G., 1995. Functional MRI evidence for adult motor cortex plasticity during motor skill learning. Nature 377, 155–158. https://doi.org/10.1038/377155a0.

Kolasinski, J., Makin, T.R., Jbabdi, S., Clare, S., Stagg, C.J., Johansen-Berg, H., 2016a. Investigating the stability of fine-grain digit somatotopy in individual human participants. J. Neurosci. 36, 1113–1127. https://doi.org/10.1523/JNEUROSCI.1742-15.2016.

Kolasinski, J., Makin, T.R., Logan, J.P., Jbabdi, S., Clare, S., Stagg, C.J., Johansen-Berg, H., 2016b. Perceptually relevant remapping of human somatotopy in 24 hours. Elife 5, 1–15. https://doi.org/10.7554/eLife.17280.

Kriegeskorte, N., Mur, M., Bandettini, P., 2008. Representational similarity analysis – connecting the branches of systems neuroscience. Front. Syst. Neurosci. 2, 1–28. https://doi.org/10.3389/neuro.06.004.2008.

Krings, T., Töpper, R., Foltys, H., Erberich, S., Sparing, R., Willmes, K., Thron, A., 2000. Cortical activation patterns during complex motor tasks in piano players and control subjects. A functional magnetic resonance imaging study. Neurosci. Lett. 278, 189–193. https://doi.org/10.1016/S0304-3940(99)00930-1.

Ledoit, O., Wolf, M., 2003. Improved estimation of the covariance matrix of stock returns with an application to portfolio selection. J. Empir. Financ. 10, 6–3621. https://doi.org/10.1016/S0927-5398(03)00007-0.

Martuzzi, R., van der Zwaag, W., Farthouat, J., Gruetter, R., Blanke, O., 2014. Human finger somatotopy in areas 3b, 1, and 2: a 7T fMRI study using a natural stimulus. Hum. Brain Mapp. 35, 213–226. https://doi.org/10.1002/hbm.22172.

Matsuzaka, Y., Picard, N., Strick, P.L., 2007. Skill representation in the primary motor cortex after long-term practice. J. Neurophysiol. 97, 1819–1832. https://doi.org/10.1152/jn.00784.2006.

Meier, J.D., Aflalo, T.N., Kastner, S., Graziano, M.S., 2008. Complex organization of human primary motor cortex: a high-resolution fMRI study. J. Neurophysiol. 100, 1800–1812. https://doi.org/10.1152/jn.90531.2008.

Merzenich, M.M., Nelson, R.J., Kaas, J.H., Stryker, M.P., Jenkins, W.M., Zook, J.M., Cynader, M.S., Schoppmann, A., 1987. Variability in hand surface representations in areas 3b and 1 in adult owl and squirrel monkeys. J. Comp. Neurol. 258, 281–296. https://doi.org/10.1002/cne.902580208.

Mogilner, A., Grossman, J.A., Ribary, U., Joliot, M., Volkmann, J., Rapaport, D., Beasley, R.W., Llinas, R.R., 1993. Somatosensory cortical plasticity in adult humans revealed by magnetoencephalography. Proc. Natl. Acad. Sci. U. S. A. 90, 3593–3597.

Mur, M., Bandettini, P.A., Kriegeskorte, N., 2009. Revealing representational content with pattern-information fMRI–an introductory guide. Soc. Cogn. Affect. Neurosci. 4, 101–109. https://doi.org/10.1093/scan/nsn044.

Nelson, A.J., Blake, D.T., Chen, R., 2009. Digit-specific aberrations in the primary somatosensory cortex in Writer's cramp. Ann. Neurol. 66, 146–154. https://doi.org/10.1002/ana.21626.

Nelson, A.J., Chen, R., 2008. Digit somatotopy within cortical areas of the postcentral gyrus in humans. Cerebr. Cortex 18, 2341–2351. https://doi.org/10.1093/cercor/bhm257.

Newmark, J., Hochberg, F.H., 1987. Isolated painless manual incoordination in 57 musicians. J. Neurol. Neurosurg. Psychiatry 50, 291–295. https://doi.org/10.1136/JNNP.50.3.291.

Norman, K.A., Polyn, S.M., Detre, G.J., Haxby, J.V., 2006. Beyond mind-reading: multi-voxel pattern analysis of fMRI data. Trends Cogn. Sci. 10, 424–430. https://doi.org/10.1016/j.tics.2006.07.005.

Nudo, R.J., Milliken, G.W., Jenkins, W.M., Merzenich, M.M., 1996. Use-dependent alterations of movement representations in primary motor cortex of adult squirrel monkeys. J. Neurosci. 16, 785–807. https://doi.org/10.1523/JNEUROSCI.16-02-00785.1996.

Oldfield, R.C., 1971. The assessment and analysis of handedness: the Edinburgh inventory. Neuropsychologia 9, 97–113.

Overduin, S.A., Servos, P., 2004. Distributed digit somatotopy in primary somatosensory cortex. Neuroimage 23, 462–472. https://doi.org/10.1016/j.neuroimage.2004.06.024.

Penfield, W., Boldrey, E., 1937. Somatic motor and sensory representation in the cerebral cortex of man as studied by electrical stimulation. Brain 60, 389–443. https://doi.org/10.1093/brain/60.4.389.

Pleger, B., Foerster, A.-F., Ragert, P., Dinse, H.R., Schwenkreis, P., Malin, J.-P., Nicolas, V., Tegenthoff, M., 2003. Functional imaging of perceptual learning in human primary and secondary somatosensory cortex. Neuron 40, 643–653. https://doi.org/10.1016/S0896-6273(03)00677-9.

Rosenkranz, K., Williamon, A., Butler, K., Cordivari, C., Lees, A.J., Rothwell, J.C., 2005. Pathophysiological differences between musician's dystonia and writer's cramp. Brain 128, 918–931. https://doi.org/10.1093/brain/awh402.

Roux, F.E., Djidjeli, I., Durand, J.B., 2018. Functional architecture of the somatosensory homunculus detected by electrostimulation. J. Physiol. https://doi.org/10.1113/JP275243.

Sanchez-Panchuelo, R.M., Francis, S., Bowtell, R., Schluppeck, D., 2010. Mapping human somatosensory cortex in individual subjects with 7T functional MRI. J. Neurophysiol. 103, 2544–2556. https://doi.org/10.1152/jn.01017.2009.

Sanes, J.N., Donoghue, J.P., Thangaraj, V., Edelman, R.R., Warach, S., 1995. Shared neural substrates controlling hand movements in human motor cortex. Science 268 (80), 1775–1777. https://doi.org/10.1126/science.7792606.

Schellekens, W., Petridou, N., Ramsey, N.F., 2018. Detailed somatotopy in primary motor and somatosensory cortex revealed by Gaussian population receptive fields. Neuroimage 179, 337–347. https://doi.org/10.1016/J.NEUROIMAGE.2018.06.062.

Schweizer, R., Voit, D., Frahm, J., 2008. Finger representations in human primary somatosensory cortex as revealed by high-resolution functional MRI of tactile stimulation. Neuroimage 42, 28–35. https://doi.org/10.1016/j.neuroimage.2008.04.184.

Schwenkreis, P., Pleger, B., Höffken, O., Malin, J.-P., Tegenthoff, M., 2001. Repetitive training of a synchronised movement induces short-term plastic changes in the human primary somatosensory cortex. Neurosci. Lett. 312, 99–102. https://doi.org/10.1016/S0304-3940(01)02196-6.

Suk, J., Ribary, U., Cappell, J., Yamamoto, T., Llinás, R., 1991. Anatomical localization revealed by MEG recordings of the human somatosensory system. Electroencephalogr. Clin. Neurophysiol. 78, 185–196. https://doi.org/10.1016/0013-4694(91)90032-Y.

Sur, M., Nelson, R.J., Kaas, J.H., 1982. Representations of the body surface in cortical areas 3b and 1 of squirrel monkeys: comparisons with other primates. J. Comp. Neurol. 211, 177–192. https://doi.org/10.1002/cne.902110207.

Tardif, C.L., Schäfer, A., Trampel, R., Villringer, A., Turner, R., Bazin, P.-L., 2016. Open science CBS neuroimaging repository: sharing ultra-high-field MR images of the brain. Neuroimage 124, 1143–1148. https://doi.org/10.1016/J.NEUROIMAGE.2015.08.042.

van Westen, D., Fransson, P., Olsrud, J., Rosén, B., Lundborg, G., Larsson, E.M., 2004. Fingersomatotopy in area 3b: an fMRI-study. BMC Neurosci. 5, 1–6. https://doi.org/10.1186/1471-2202-5-28.

Waehnert, M.D., Dinse, J., Schäfer, A., Geyer, S., Bazin, P.-L., Turner, R., Tardif, C.L., 2016. A subject-specific framework for in vivo myeloarchitectonic analysis using high resolution quantitative MRI. Neuroimage 125, 94–107. https://doi.org/10.1016/J.NEUROIMAGE.2015.10.001.

Walther, A., Nili, H., Ejaz, N., Alink, A., Kriegeskorte, N., Diedrichsen, J., 2016. Reliability of dissimilarity measures for multi-voxel pattern analysis. Neuroimage 137, 188–200. https://doi.org/10.1016/j.neuroimage.2015.12.012.

Weise, D., Gentner, R., Zeller, D., Nagel, A., Reinsberger, C., Rumpf, J.J., Classen, J., 2012. Focal hand dystonia: lack of evidence for abnormality of motor representation at rest. Neurology 78, 122–128. https://doi.org/10.1212/WNL.0b013e31823efce6.

Wiestler, T., McGonigle, D.J., Diedrichsen, J., 2011. Integration of sensory and motor representations of single fingers in the human cerebellum. J. Neurophysiol. 105, 3042–3053. https://doi.org/10.1152/jn.00106.2011.

Woolsey, C.N., Settlage, P.H., Meyer, D.R., Sencer, W., Pinto Hamuy, T., Travis, A.M., 1952. Patterns of localization in precentral and "supplementary" motor areas and their relation to the concept of a premotor area. Res. Publ. Assoc. Res. Nerv. Ment. Dis. 30, 238–264.

Yokoi, A., Arbuckle, S.A., Diedrichsen, J., 2018. The role of human primary motor cortex in the production of skilled finger sequences. J. Neurosci. 38, 2798–17. https://doi.org/10.1523/JNEUROSCI.2798-17.2017.

Yousry, T.A., Schmid, U.D., Alkadhi, H., Schmidt, D., Peraud, A., Buettner, A., Winkler, P., 1997. Localization of the motor hand area to a knob on the precentral gyrus. A new landmark. Brain 120 (Pt 1), 141–157. https://doi.org/10.1093/brain/120.1.141.